Published by SET Publisher

Journal of Basic & Applied Sciences

ISSN (online): 1927-5129

Effects of Magnetized, Chelated Iron Foliage Treatments, and Metal Halide Lamps on Plant Water Structure, Water Vapor Dynamics, and Resilience for Legumes under Water Stress

Craig Ramsey*

Retired Fort Collins, CO 80526, USA

Article Info:

Keywords:
Structured Water,
Deficit Irrigation,
Abiotic Stress,
Resilience,
Plant Defenses,
Infrared Lamps,
Water Conservation,
Crop Drought Tolerance.

Timeline:
Received: April 05, 2024
Accepted: May 01, 2024
Published: May 24, 2024

Citation: Ramsey C. Effects of Magnetized, Chelated Iron Foliage Treatments, and Metal Halide Lamps on Plant Water Structure, Water Vapor Dynamics, and Resilience for Legumes under Water Stress. J Basic Appl Sci 2024; 20: 59-80.

DOI: https://doi.org/10.29169/1927-5129.2024.20.06

*Corresponding Author
E-mail: clramsey37@gmail.com

Abstract:

A greenhouse study was conducted to determine the effects of foliar applications of magnetized, chelated liquid iron fertilizer for increasing the drought tolerance of two legumes. The study objectives were to determine the drought tolerance effects of four treatments on foliar gas exchange, soil moisture, and plant growth for soybean (*Glycine max) and velvet bean (Mucuna pruriens*) plants. The plant treatments included applications with chelated liquid iron fertilizer (2.5 and 5%) with a conventional boom sprayer, with and without magnets in the spray lines, and metal halide lamps. Three gas exchange measurements were collected before applying the foliage treatments and after two water stress treatments. A foliage and metal halide lamp treatment deactivated or unlinked nine interconnected gas exchange parameters that are correlated with plant defense activities during water stress conditions. The deactivation of interconnected regulatory gas exchange functions improved metabolic efficiency, reduced stress levels, and boosted plant resilience to abiotic stressors. Also, the study findings suggest that the study treatments maintained or increased the level of biologically structured water in plant tissues and vascular systems.

1. INTRODUCTION

This follow-up article proceeds from an original article published by Ramsey [1] involving a greenhouse study with foliar spray treatments on soybean (*Glycine max) and* velvet bean *(Mucuna pruriens*) plants. This follow-up article presents new findings from unexplored data and analysis from the study. The unexplored data was re-analyzed due to the inclusion of a new study factor involving a change in the lighting systems used in this study. The latest analysis also includes several new gas exchange responses, such as saturated vapor pressure (SVTleaf) and mole fraction of water in the intercellular airspaces within the leaves. Also, the discussion section includes a short review of the effects of light quality and spectral bands on bound water content in plants. This review adds credence to the challenging findings presented in this study. The short review includes structured water terms such as bound water, exclusion zone (EZ) water, and biologically structured water (BSW) that are considered synonymous with each other.

The study design included two separate gas exchange collection dates after the single foliage spray treatment. The second gas exchange collection date occurred after all the plants were moved into another greenhouse bay that provided full control of the lighting and cooling systems. The change in greenhouse bays, with the new lighting system in the second bay, was not fully understooduntil recent publications of infrared radiation and water structure research emerged. This article investigated the effects of the second bay lighting system on several gas exchange parametersrelated to water vapor and water properties within plants. Also, if the lighting system in the second bay increased water structure in the plant vascular system and foliage tissue, an increase in structured water levels should also affect plant regulatory defenses based on the Ramsey study findings [2-3].

During literature search on infrared lamps and biologically structured water (BSW) water, this author discovered that metal halide lamps used in greenhouses also emitted biologically significant levels of infrared radiation across all three major IR bands and visible light. Most of the literature on greenhouse lighting systems focuses on the Photo synthetically Active Radiation (PAR) wavelengths (400 to 700 nm) used in photosynthesis. The High-Intensity Discharge (HID) metal halide (MH) lamps used in the second bay also emit UV and IR radiation. Until recently, the vast majority of greenhouse lamp and lighting literature ignored these non-visible light wavelengths because these frequencies were assumed to have minor effects on plant tissue or functions. However, in the past 10-15 years, plant research has started to investigate the effects of IR spectral bands on water transport, gas exchange, and BSW water levels in plants. The literature findings also show that mid to far IR radiation significantly improves plant health and growth, and these findings were included in the discussion section.

The interrelationships between water vapor pressure dynamics within leaves, leaf temperature, and atmospheric conditions are complex and highly interconnected [15-17]. Gas exchange analysis involved the following water vapor variables: leaf vapor pressure deficit (vpdl), saturated vapor pressure in the leaf (SVTleaf), saturated vapor pressure in air (SVTair), water vapor concentration inside the leaf (h2o_l), difference in water vapor concentration between inside leaf and the air (h2o_diff), air temperature (tair), and leaf temperature (Tleaf).

The spongy mesophyll inside of leaves contains intercellular airspaces near the stomatal openings, allowing water vapor to exit the stomata to cool the plants [18-19]. These intercellular airspaces contain water vapor and CO_2, and these variables can be measured in units of pressure (kPa) or units of mole fractions (mol H_2O or CO_2/ mol air). Water vapor pressure inside the leaf determines the rate at which water transitions from liquid to vapor. The higher the vapor pressures at a given temperature, the weaker the H-bonds in the liquid water, and evaporation rates increase [3]. Foliage evaporation rates are a function of the Leaf Vapor Pressure Deficit (vpdl in kPa),which is the difference in the air's Saturated Vapor Pressure (SVTair) and Relative Humidity (RH) outside of the leaf [17-19].

The original study hypothesis and data analysis were reported in the article by Ramsey [1]. Analysis of the data in this article is based on two new hypotheses. The first hypothesis states that combining the foliage treatments with the lighting system in the second greenhouse bay would improve gas exchange responses to the second water stress treatment. The second hypothesis states that combining foliage and lighting system treatments would reduce or deactivate several regulatory interconnections among gas exchange parameters that are typically used to reduce the risk of excessive water vapor losses during water stress. The second hypothesis was derived and formulated from the results of another water stress article by Ramsey [3].

2. MATERIAL AND METHODS

2.1. Study Design

A greenhouse study was conducted at the USDA-APHIS laboratory in Fort Collins, CO, to determine the effects of four foliar treatments containing a series of magnetized/non-magnetized, chelated iron solution son two C3 legumes. The original study factors included two legume species, two sprayer systems (magnetized and non-magnetized spray booms), two chelated iron fertilizer rates (2.5 and 5% v/v), and three measurement dates. Also, the lighting system used in the second water stress treatment was an additional study factor in the data analysis.

The two legume species selected were velvet bean (*Mucuna pruriens*),a tropical legume, and soybean (*Glycine max*), a temperate legume. Five replicates were used for the velvet bean plants (VB), and four replicates were used for the soybean plants (SB) for each of the four application treatments. Foliar gas exchange and volumetric soil moisture (m^3/m^3) data were collected to determine the legume responses to two water stress treatments.

2.2. Seed Planting and Soil Mixture Description

Velvet bean and soybean seeds were germinated in plastic trays and allowed to grow into 5-10 cm seedlings. The most vigorous seedlings were then transplanted into 1.5 L plastic pots using a 50:50 mix of potting soil and sand. These seedlings were finally culled to the most vigorous seedling that survived transplanting. The soil mixture was 50% sand and 50% potting soil (Fafard 4M mixed with Sphagnum peat moss and vermiculite).

2.3. Greenhouse Light System and Water Stress Treatments

The plants were grown in two different greenhouse bays for this study. The first bay was a fan-cooled greenhouse bay with the seedlings grownunder ambient sunlight. The first bay had supplemental, grow light lamps for a 14 and 10-light:dark photoperiod. The four foliar treatments were applied and allowed to be absorbed and translocated into the foliage and vascular system for nine days. Following the foliage treatment, the first deficit irrigation treatment was initiated by reducing soil moisture levels from 0.37 m^3/m^3 to 0.19 m^3/m^3 over a five-day event. Gas exchange responses and soil moisture data were collected over nineteen days to measure plant responses during the sustained water stress event. Soil moisture was maintained at target levels by monitoring the daily soil moisture losses and replacing the average water loss with a measured volume of water daily.

The plants were transferred to a second bay after collecting the gas exchange data for the first water stress treatment. The plants were transferred to a fully controlled bay to complete the gas exchange measurements under the second water stress treatment. After the baseline and first gas exchange measurements, the plants were hand-watered back to field capacity. The plants were then moved into the second temperature and light-controlled greenhouse bay with height-adjustable metal halide lamps. All plants were adjusted to the light intensity for six days. The greenhouse lamps were adjusted in height above the plants so that plants received 500 $\mu mol/m^2/s^1$of light for a 9 and 14 h light: dark photoperiod. The fans were controlled, so the temperature in the second baywas nearly uniform at 27 C during the day.

The second water stress treatment was completed in five days, following the six-day adjustment to the second greenhouse bay. Volumetric soil moisture levels were reduced from an average of 0.38 m^3/m^3(38 %) down to 0.22 m^3/m^3(22%), and the plants adapted to the new deficit irrigation treatment over five days. Gas exchange responses and soil moisture data were collected over the next eight days. The foliar biomass was harvested at the end of the second deficit irrigation event to determine the plant growth responses to the study treatments.

2.4. Sprayer Description

The CO_2 backpack sprayer (R&D Sprayers, Opelousas, LA)had a six-nozzle, 3.4 m boom. The spray pressure was 310 kPa, and the total spray volume was 701 l/ha. The nozzles were TeeJet XR 8003 VS, producing a droplet with a volume median diameter of 285 microns. Nozzles were spaced 46 cm apart, and nozzle height above the plants was approximately 41 cm. Half of the six-nozzle boom was fitted with three nozzles fed with magnetized spray hoses. The other half of the boom was fitted with three nozzles fed with non-magnetized spray hoses.

The magnetized spray hoses had cylindrical neodymium magnets inserted into the three hose sections between the three nozzles. The magnets (grade N-52) were hollow, allowing the spray solution to be magnetized as it passed through each

magnetized section of the boom. Magnetswere axially magnetized, i.e., magnet poles were at the ends of the magnets, and magnet size was 19 x 19 mm with a 6.4 mm inside diameter. There were 36 magnets in the three hoses in the magnetized half of the boom. The magnetic field strength was 560 mT (0.56 Tesla) when measured on the end of one magnet at the end of a string of fourteen magnets inserted in a single hose section. Each of the six nozzles was adjusted and calibrated to deliver a flow rate of 18.3 ml/s.

2.5. Plant Fertilizer and Chelated Iron Fertilizer Description

The liquid fertilizer contained nitrogen, phosphorous, and potassium (NPK) plus micronutrients, a surfactant, and two rates of chelated iron fertilizer. The N-P-K fertilizer (Jack' Classic, JR Peters, and Allentown, PA) was mixed with water at 7.5 ml/l. The surfactant (Silwet L-77, Phyto Tech Labs, Lenexa, KS) was mixed at 0.2% (v/v) for all four treatments.

The chelated iron fertilizer (Iron & Soil Acidifier, Green Light, San Antonio TX)used as a study factor contained sulfur-3.1%, copper-0.12%, iron-4.6%, and zinc-0.12%, and was mixed at either 2.5 or 5% (v/v).The fertilizer had a Fe concentration of 4.6% and contained ferric ($Fe3^{+}$) ions chelated with N-hydroethylene diaminetriacetic acid (HEDTA) trisodium salt. The four spray solutions included two magnetic foliar applications with 2.5 or 5% iron fertilizer and two non-magnetic applications with 2.5 or 5% iron fertilizer.

2.6. Plant Gas Exchange Description

Baseline gas exchange data was collected 12 days before the chelated iron fertilizer treatments were applied to the foliage. Velvet bean seedlings were 69 days old, and the soybeans were 90 days old during the chelated iron fertilizer applications. The first and second gas exchange measurements started 17 and 59 days after the iron fertilizer treatments, respectively. Plant and soil data collection included three measurement dates for gas exchange sampling, two soil moisture readings, and a final foliar harvest to determine oven-dry stem and foliar biomass. The three gas exchange readings included a baseline measurement before the foliar application, a second data collection after the first water stress treatment, and a third measurement after the second water stress treatment.

A gas exchange instrument (LICOR 6400 XT, LI-COR Environmental, and Lincoln, NE) was used for all foliage gas exchange measurements. During the baseline and first gas exchange measurement date, the 6400 XT was set for Photo synthetically Active Radiation(PAR) = 200 µmol/m^2/s^1, CO2 concentration = 400 mg/l, airflow rate = 300 µmol/s, and block temperature = 30 C across all treatments. During the second gas exchange measurement date, the 6400 XT was set for PAR = 500 µmol/m^2/s^1, CO2 concentration = 400 mg/l, airflow rate = 500 µmol/s, and block temperature = 30 C across all treatments. The uppermost, fully mature leaves were selected for gas exchange measurements. Three leaves per plant were selected: dark green or mature leaves with no disease spots inside the measurement area. All gas exchange measurements include six replicates (4 or 5 plants x 3 leaves = 12 or 15 replicates per treatment) that was included with the extra replicate runs due to hidden replication. Soil moisture data was collected along with the gas exchange parameters, and all the parameters were combined into a single dataset so that soil moisture could be tested as a covariate in the data analyses.

2.7. Spectral Output for the LED and HID- MH Lamps

Two lighting systems were used while taking the three gas exchange measurements with the LICOR 6400 XT. The first lighting system used for the baseline and first measurement date was an LED lamp (Pro Max Grow, Tappan, NY). The plants were under ambient sunlight until approximately 15 min from gas exchange measurements. Then, they were placed under the LED lamp to ensure all the plants were exposed to a uniform light source for approximately 15 min. before taking the gas exchange measurements. The LED lamp was about 25 to 45 cm above the top of the plants to ensure the foliage had uniform light conditions during the gas exchange measurements. The LED lamp used 125 watts and had 384 red and blue diodes. The PAR output of the LED and HID-MH lamps for the three gas exchange measurements are listed in Table **2**. The spectral output for the Pro Max lamp is graphed in Figure. **1**.

The second lighting system used in the second greenhouse bay included a bank of 1,000-watt High Intensity Discharge (HID) metal halide (MH) lamps. These lamps measured gas exchange for the second water stress treatment. The HID MH lamps used in this study were replaced with LED lamps, and the manufacturer details were not saved for those lamps. The HID MH lamps used in the second bay most likely

had a PAR spectral band similar to generic MH bands listed on several websites [21] (Figure. **2**). Most HID-MH lamps are operated at higher wattage (≥ 1,000 watts) to enhance the red band regions in the visible light spectrum to boost plant growth. In addition, HID MH lamps also emit ultraviolet and infrared radiation. A metal halide lamp used in a Zeiss microscope emits about 10% ultraviolet light, about 45% visible light, and about 20% infrared radiation with 10% loss due to resistive heating [22]. These non-visible light spectral bands are probably representative of most HID MH lamps. Krizek *et al*. [23] compared the visible and infrared spectral output of two greenhouse lamps: High-Pressure Sodium (HPS) and a combination of HPS and MH bulb systems (HPSMH lamps). They measured several spectral bands for the combination HPSMH system: 1) 290-800 nm (233 w/m^2), 2) 800-3,000 nm (189 w/m^2), 3) 2,900-3,000 nm (422 w/m^2), and 3,000-50,000 nm (49 w/m^2) [23], The second band from 800 to 3,000 nm wavelengths includes the near (780-1,400 nm) and mid-infrared (1,400-3,000 nm) bands. The fourth band (3,000 to 50,000 nm) covers the far infrared bands emitted from the HPS:MHlamp system. The combination HPS:MH system radiated a total energy of893 w/m2 9 (4,108 µmol/m^2/s) between the NIR to FIR infrared bands and 225 µmol/m2/s in the FIR band alone.

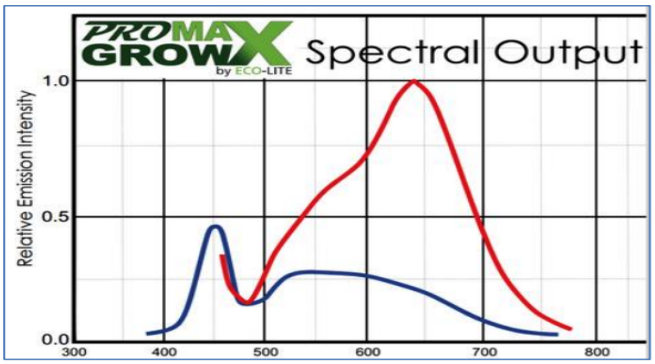

Figure 1: PAR spectral output for Pro Max LED lamp [20].

Little information has been published on the UV and IR spectral band output of HPS and HID MH lamps, as it was assumed that those bands had little effect on plant functions. Plant research focused on the effects of visible PAR wavelengthson plant physiology, metabolism, and growth. It was commonly known that plants reflected most near-infrared wavelengths, making that IR spectral band unimportant. Also, it was known that mid or short-wave infrared wavelengths were only absorbed by water in the tissue, which was also assumed to be of no interest with insignificant effects on foliage functions. The IR review in the discussion section shows that these unfounded assumptions could lead to erroneous results. Recent findings show that IR radiation significantly affects plant water content and water-based physiological functions as well as overall plant health and growth.

Also, the UV and IR bands require specialized spectrographic meters to delineate each band, which are only found in well-equipped labs.Before the introduction of LED lamps, the two most common lighting in commercial greenhouses were HPS and HID MH lamps [24]. These lamp systems consume large amounts of electricity and arevery expensive to operate under greenhouse and hydroponic conditions. LED lighting systems are much less costly and have been adopted by virtually all food and horticultural production systems that rely on lighting systems to grow plants

The average temperature inside the arc tube in an MH lamp is approximately 2,000 F. This temperature converts into a peak wavelength of 2,121 nm, or within the mid-infrared band (1,400-3,000 nm), based on Wein's law [25]. Water in plant tissue is preferentially absorbed by the short wave IR (SWIR) wavelengths of 1,400, 1,900, and 2,400 nm [26].Thus, the HID MH lamp radiation signature probably peaked in the SWIR spectral bands,which is the same IR band for optimal plant water absorption. All HID MH lamps produce intense heat, and the manuals offer safety warnings to avoid lamp damage from high temperatures. Radiation from HID MH lamps that raises temperatures equates to transmitting infrared energy bands. In summary, HID MH lamps radiate SWIR wavelengths with optimal water absorption rates, with a high probability of increasing water structure in sap and inter/intracellular water content. In contrast, LED lamps don't emit any wavelengths outside the visible light spectrum.

2.8. Soil Moisture Methods

Volumetric soil moisture (SM) readings were collected with data loggers and soil moisture and temperature sensors (ECH2O data logger and 5-TM soil sensors, METER Environmental, Pullman, WA). The soil probes were 5 cm in length. The probes were pushed into the soil surface to measure soil moisture between 5 to 10 cm from the surface. During the three gas exchange measurements, soil moisture was measured for one data point for each treatment. The SM data was compiled with the gas exchange data so that it could be used as a covariate in the gas exchange analysis. Also, soil moisture was measured on a 24-hour basis during the second water stress test using the same 5 cm

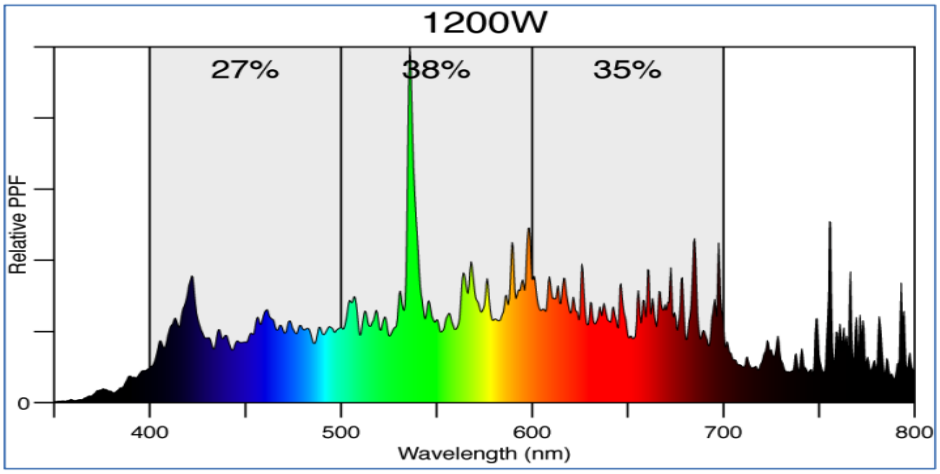

Figure 2: The Photosynthetic Active Radiation (PAR) spectral bands of a 1200-watt metal halide lamp [21].

probes. The SM data was collected at one-hour intervals to estimate evapotranspiration rates over 24 hours for each treatment. Soil evapotranspiration rates were calculated by converting volumetric soil moisture (m^3/m^3) into evapotranspiration rates (ml/h/pot), using the average volume of soil in each pot (1,340 ml or 0.00134 m^3). Average hourly moisture losses were calculated from the 24-hour data. All plants were watered once a day in the morning, and soil moisture was monitored daily to determine the overall water use/loss between watering cycles.

2.9. Analysis

Data were analyzed using a repeated measure model, as it was a longitudinal study with the same plants measured over time for the baseline and two deficit irrigation events. The first data collection occurred before the plants were treated to provide the baseline plant responses. Two tables reported a set of predicted baseline means for selected gas exchange parameters to compare plant responses before and after the first and second water stress treatments .Gas exchange data used the SAS JMP (SAS Institute Inc., Clary, NC) Restricted Maximum Likelihood (REML) model for the repeated measures analyses. The REML model was restricted to two-way interaction terms to take advantage of hidden interactions. The JMP Standard Least Squares model was used to test the treatment effects on foliar biomass and evapotranspiration analysis. Analysis results were deemed to be significant if *p*-values were less than 0.05. Error bars in graphs represent the standard error of model values.

Multivariate analyses were conducted to correlate any relationships among six gas exchange parameters. Multivariate pairwise correlation tested the interconnectivity among the gas exchange parameters. The correlation tests provided insight into the regulatory functions of plant defense activities for water-stressed plants. Regression analysis tested the relationships between vapor pressure deficit and the mole fraction of water vapor inside the leaves. Regression analysis tested the relationships betweenthe reciprocal of WUE(1/WUE) and stomatal conductance for the three gas exchange measurements.

3. RESULTS

The average PAR readings inside (PARi) and outside (PARo) for the three gas exchange dates were summarized in Table. PAR measurements were taken with light sensors inside and outside the sample chamber to report the averages for the mean, minimum, and maximum values for the baseline, first, and second gas exchange dates. The outside PAR (PARo) values show the range in light intensity the plants were exposed to for 14 hours per day in the first bay and nine hours in the second bay.The visible light PAR values differed between the two lighting systems in each bay.In addition to the PAR reading in Table **1**, each HID MH lamp in the second bay also radiated 225 µmol/m^2/s in the FIR band and 4,108 µmol/m^2/s across the whole IR band for nine hours, using the IR results from the Krizek *et al*. study [23].The effect of IR radiation on water dynamics in plants will be discussed in the gas exchange results below.

Multivariate analysis was conducted on eight gas exchange parameters for the baseline of soybean and velvet bean plants and the first and second water stress treatments(Table **2-3**). The results for the baseline correlation test show approximately 14 and 12

Table 1: Photosynthetic Active Radiation (PAR) for Three Gas Exchange Measurement Dates. The Baseline and First Measurement Dates Used the LED Lamps, and the Second Date Used the HID MH Lamp

Measuring Date	Mean (PARi)[a]	Mean (PARo)[b]	Min (PARi)	Min (PARo)	Max (PARi)	Max (PARo)
	μ mol/m^2/s					
Baseline	199	269	198	74	200	689
LED lamp	198	194	198	46	200	382
HID MH lamp	502	524	498	104	505	1220

[a]PARi = PAR inside the leaf chamber, [b] PARo = PAR outside the leaf chamber, Mean = Ave. PAR across the measurement date, Min = Minium PAR across the measurement date, Max = Maximum PAR across the measurement date.

significant pairwise correlations for the soybean and velvet bean plants, respectively (Tables **2-3**). Several pairwise correlations with p-values <.0001 indicate perfect correlation that implies that parameter calculations contained confounding variables such as temperature in the underlying equations. These "perfect" correlations should be ignored.

The baseline pairwise correlation tables show high interconnectivity among leaf, water vapor, and atmospheric gas exchange parameters. This interconnectivity reflects the complex regulatory plant defense system, which is necessary for balancing plant growth with the risk of plant injury due to excessive water vapor losses for plants under moderate water stress. The repeated measures analysis reveals that gas exchange dynamics changed across the data collection dates compared to the baseline correlations.

Pairwise correlations tested the effects of the foliage treatments combined with the effects of the first water stress treatment nine days after foliage applications for both species (Tables **2-3**). Data analyses for the first water stress treatment show positive and negative correlations due to foliage treatments and a reduction in soil moisture of 48 and 37% for the soybean and velvet bean plants, respectively. The interconnectivity and correlations among gas exchange responses to both the foliage and watering treatments areevident when comparing the baseline and first water stress events correlation *p*-values for both species. In general, the analyses show that most of the pairwise tests that were significant for the baseline plants were also significant after the foliage treatment and first water stress treatment.

There were 27 possible pairwise tests among all the baseline and second water stress parameters (Tables **2-3**). Nine of these 27 pairwise correlations were converted from significant to non-significant values when comparing baseline and second water stress *p*-values. In other words, nine gas exchange parameters that were interrelated and significantly correlated in the baseline data became non-significant and non-correlated for the second water stress *p*-values. The lack of significance implies that the regulatory functions of the interconnected gas exchange parameters were deactivated by the foliage treatments combined with the HID MH lamps in the second bay. These same nine pairwise correlations were also converted from significant to non-significant and non-correlated results in the Ramsey study in Tables **6-7** for the velvet bean species [3].

Analysis of baseline data shows an indirect relationship between stomatal conductance and vpdlfor soybeans (Figure **3** upper graph). Also, there was an indirect relationship between transpiration and vpdl for soybean plants but no relationship for velvet bean plants (Figure **3** lower graph).

Baseline regression for transpiration and vpdl for velvet bean in this study shows no relationship (*p*-value 0.2328) (Figure **3**). This relationship is not in agreement with the soybean regression findings (*p*-value 0.0020) (Figure **3**). These inconsistent findings could be rechecked by analyzing the same gas exchange relationships in the Ramsey study [3]. The relationship between transpiration and vpdl for the Ramsey studywas analyzed to determine if the two studies agreed with each other (Figure **4**). Comparison of the two linear regressions shows disagreement in the *p*-value results. This study shows no relationship between transpiration and vpdl (*p*-value 0.2328) (Figure **4**). The medium soil moisture regression for the Ramsey study shows a strong negative relationship (*p*-value <0.0001) (Figure **4**) which agrees with the soybean results in this study (Figure **3** lower graph). However, the transpiration and vpdl relationship turns

Table 2: Multivariate Correlations and *P*-Values for Eight Gas Exchange Parameters for Soybean Plants for Baseline and First and Second Water Stress Measurement Dates

Variable	by Variable	Baseline Correlation	Signif Prob (*p*-value)	First Water Stress Correlation	Signif Prob (*p*-value)	Second Water Stress Correlation	Signif Prob (*p*-value)
Trans	S Cond	0.8982	<.0001	0.9978	<.0001	0.9649	0.0001
Tair	S Cond	0.1464	0.3207	-0.8085	0.0026	0.0083	0.9845
Tair	Transp	-0.0898	0.5439	-0.7739	0.0052	0.0507	0.905
Ltemp	S Cond	-0.3637	0.0111	-0.7858	0.0041	-0.5922	0.1219
Ltemp	Transp	-0.5837	<.0001	-0.7517	0.0076	-0.5998	0.116
Ltemp	Tair	0.8227	<.0001	0.9931	<.0001	0.7436	0.0344
RH	S Cond	0.515	0.0002	-0.462	0.1526	-0.5984	0.1171
RH	Transp	0.2099	0.1521	-0.437	0.179	-0.7633	0.0275
RH	Tair	0.7196	<.0001	0.7884	0.0039	0.2102	0.6173
RH	Ltemp	0.4062	0.0042	0.819	0.002	0.712	0.0476
SVTleaf	S Cond	-0.3673	0.0102	-0.7908	0.0038	-0.5974	0.1178
SVTleaf	Trans	-0.5866	<.0001	-0.7567	0.007	-0.6055	0.1116
SVTleaf	Tair	0.8225	<.0001	0.9942	<.0001	0.7385	0.0364
SVTleaf	Ltemp	0.9998	<.0001	0.9997	<.0001	1	<.0001
SVTleaf	RH	0.4065	0.0041	0.8099	0.0025	0.716	0.0458
SVTair	S Cond	-0.262	0.0721	-0.7948	0.0035	-0.5082	0.1985
SVTair	Trans	-0.4922	0.0004	-0.7606	0.0066	-0.5074	0.1993
SVTair	Tair	0.8889	<.0001	0.9964	<.0001	0.8178	0.0131
SVTair	Ltemp	0.9916	<.0001	0.9993	<.0001	0.9929	<.0001
SVTair	RH	0.4904	0.0004	0.8073	0.0027	0.6508	0.0805
SVTair	SVTleaf	0.9916	<.0001	0.9997	<.0001	0.992	<.0001
H2O_l	S Cond	0.4825	0.0005	-0.7009	0.0163	-0.5951	0.1196
H2O_l	Trans	0.1771	0.2286	-0.6724	0.0234	-0.7561	0.03
H2O_l	Tair	0.7506	<.0001	0.9397	<.0001	0.2495	0.5513
H2O_l	Ltemp	0.4522	0.0013	0.9406	<.0001	0.7375	0.0368
H2O_l	RH	0.9982	<.0001	0.9351	<.0001	0.9992	<.0001
H2O_l	SVTleaf	0.4527	0.0012	0.9375	<.0001	0.7413	0.0353
H2O_l	SVTair	0.5346	<.0001	0.9395	<.0001	0.6798	0.0636

[a]Trmmol = transpiration, Cond = stomatal conductance, tair = air temperature, Ltemp = leaf temperature, RH = relative humidity in sample chamber, SVTleaf = saturated vapor pressure in leaf, SVTair = saturated vapor pressure in air, h2o_l = water vapor concentration inside leaf.

Table 3: Multivariate Correlations and *P*-Values for Eight Gas Exchange Parameters for Velvet Bean Plants for Baseline and First and Second Water Stress Measurement Dates

Variable	by Variable	Baseline Correlation	Signif Prob (*p*-value)	First Water Stress Correlation	Signif Prob (*p*-value)	Second Water Stress Correlation	Signif Prob (*p*-value)
Trans	S Cond	0.9183	<.0001	0.9953	<.0001	0.9457	<.0001
Tair	S Cond	-0.3091	0.0163	0.3929	0.1474	0.2578	0.335
Tair	Transp	-0.1925	0.1406	0.3224	0.2412	0.2428	0.3649
Ltemp	S Cond	-0.6562	<.0001	-0.3384	0.2173	-0.4343	0.0928
Ltemp	Transp	-0.5906	<.0001	-0.4019	0.1376	-0.4455	0.0838
Ltemp	Tair	0.8986	<.0001	0.6851	0.0048	0.7422	0.001
RH	S Cond	-0.1109	0.3989	-0.8648	<.0001	0.3339	0.2062

(Table 3). Continued.

Variable	by Variable	Baseline Correlation	Signif Prob (p-value)	First Water Stress Correlation	Signif Prob (p-value)	Second Water Stress Correlation	Signif Prob (p-value)
RH	Transp	-0.4405	0.0004	-0.9057	<.0001	0.0801	0.7682
RH	Tair	0.0019	0.9885	0.024	0.9324	0.4567	0.0753
RH	Ltemp	0.173	0.1862	0.6469	0.0091	0.2716	0.3089
SVTleaf	S Cond	-0.6562	<.0001	-0.3375	0.2186	-0.4334	0.0935
SVTleaf	Trans	-0.5918	<.0001	-0.4009	0.1386	-0.4463	0.0831
SVTleaf	Tair	0.8977	<.0001	0.6852	0.0048	0.7424	0.001
SVTleaf	Ltemp	0.9999	<.0001	1	<.0001	0.9999	<.0001
SVTleaf	RH	0.1758	0.1791	0.6456	0.0093	0.2723	0.3075
SVTair	S Cond	-0.5965	<.0001	-0.1888	0.5003	-0.298	0.2623
SVTair	Trans	-0.5202	<.0001	-0.2576	0.3539	-0.3116	0.2401
SVTair	Tair	0.9338	<.0001	0.798	0.0004	0.8351	<.0001
SVTair	Ltemp	0.996	<.0001	0.9857	<.0001	0.9885	<.0001
SVTair	RH	0.1429	0.276	0.5404	0.0376	0.3268	0.2167
SVTair	SVTleaf	0.9959	<.0001	0.9857	<.0001	0.9885	<.0001
H2O_I	S Cond	-0.1192	0.3643	-0.8526	<.0001	0.3416	0.1954
H2O_I	Trans	-0.4378	0.0005	-0.8955	<.0001	0.0991	0.715
H2O_I	Tair	0.0931	0.4791	0.0525	0.8526	0.5346	0.0329
H2O_I	Ltemp	0.2461	0.0581	0.666	0.0067	0.3339	0.2063
H2O_I	RH	0.9949	<.0001	0.9996	<.0001	0.996	<.0001
H2O_I	SVTleaf	0.2487	0.0553	0.6647	0.0069	0.3346	0.2053
H2O_I	SVTair	0.2209	0.0899	0.5628	0.029	0.3954	0.1295

[a]Trmmol = transpiration, Cond = stomatal conductance, tair = air temperature, Ltemp = leaf temperature, RH = relative humidity in sample chamber, SVTleaf = saturated vapor pressure in leaf, SVTair = saturated vapor pressure in air, h2o_I = water vapor concentration inside leaf.

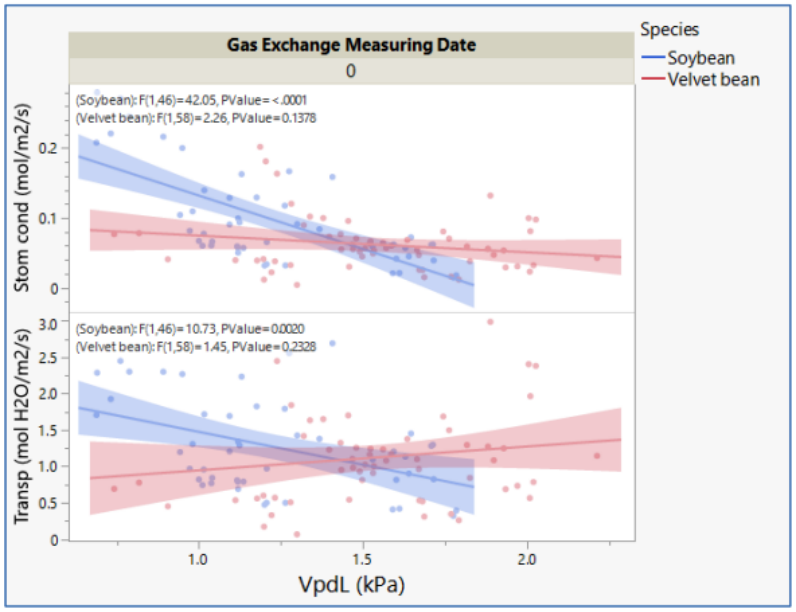

Figure 3: Baseline linear relationship between stomatal conductance and vpdl by species (top graph). Baseline linear relationship between transpiration and vpdl by species (bottom graph). Baseline (0) gas exchange measurement date (upper x-axis) and species (legend) and regression *p*-values by species (text inside graphs).

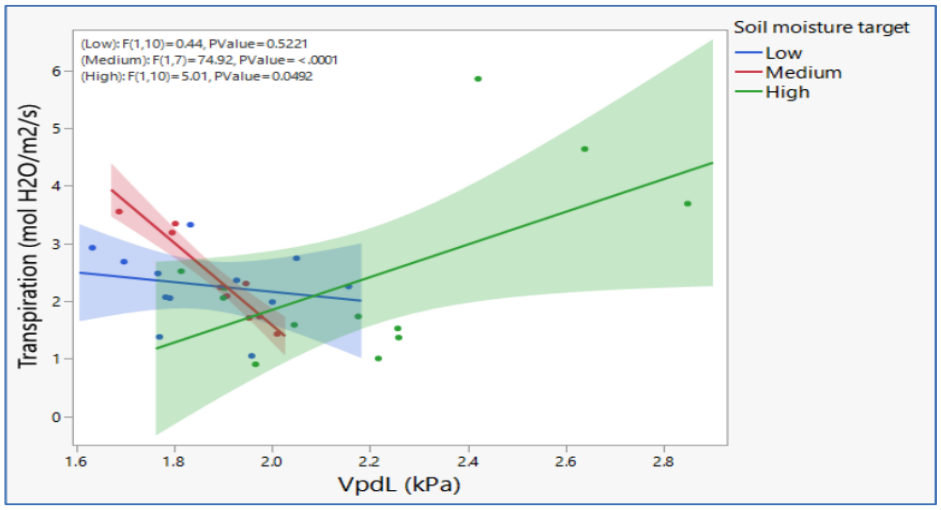

Figure 4: Linear regression for transpiration by vpdl for velvet bean in the Ramsey study [3]. Regression for control treatment only for three soil moisture targets (legend).

positive (*p*-value 0.0492) for the high soil moisture target (Figure **4**). This discrepancy in findings for the baseline and control treatments between the two studies is probably due to the mite infestation in the velvet bean plants during the second water stress treatment. The mites reduced sap flow,which altered transpiration rates enough to negate the normal negative relationship between transpiration and vpdl.

For soybeans, the baseline analysis showed a negative relationship between transpiration and vpdl (*p*-value = 0.002) (Figure **3**). This relationship became insignificant (*p*-value = 0.0547) (Figure **5**) for soybeans after the second water stress treatment. The reversion of the relationship from negative significance to non-significance implies that transpiration became unlinked with vapor pressure deficit due to the effects of the study factors and HID MH lamps during the second water stress treatment. The reversion ofregression results for soybeansagrees with the reversion in multivariate findings in the Ramsey study [3]between the control and optimal treatments study for velvet beans in Tables **6-7** reported in the Ramsey article.

There was anegative linear relationship between the mole fraction of water vapor in the intercellular airspaces (H2O_leaf) and vapor pressure deficit based on leaf temperature (vpdl) for this study (Figure **6A**), and the Ramsey study [3] (Figure **6B**). Both linear regressions were run on the raw data in both studies and across several treatments to validate the strong negative relationship in both studies. The predicted gas exchange parameters estimated by the REML models are the most accurate, but they don't provide any data points to run a reliable regression test. Regression analysis of the raw data results in less accurate models but provides a more reliable regression model due to the multiple data points for each parameter.

Regression analysis also shows a negative relationship between H2O-leaf and vpdl for both studies (Figure **6A**, **6B**). In other words, as the mole fraction of water vapor in the intercellular airspaces increases, there is a reduction in the vapor pressure deficit for the leaf. The discussion section in the article by Ramsey [3] explains that the physical properties of BSW water are related to the increase in the mole fraction of water vapor in the intercellular airspaces. Any plant treatments that increase the BSW water levels in plant tissue or foliage also enhance water properties such as vapor pressure, latent heat of vaporization, and ion exclusion. These BSW water properties likely explain the unexpected improvement in many gas exchange responses to the water stress treatments.

The linear relationship between H2O_leaf and vpdl (Figure **6B**) shows that an increase in the mole fraction of water vapor reduces the vapor pressure deficit and plant stress levels. The equation in Figure **6B** was used to estimate the effects of H2O_leaf on vpdl for the Ramsey study [3]. The predicted gas exchange values in Table **11** [3] show that H2O_leaf increased by 19 mmol H_2O/mol air from the control to optimal treatment for the low soil moisture target. This increase in water vapor mole fraction reducedvpdl from 3.66 to 2.14 kPa or a 1.52 reduction in kPa. In this study, H2O_leaf increased by 4.6 mmol H_2O/mol air from the baseline to the magnetized spray, and 5% Fe was used for the second water stress test (Figure **6A**). This increase in H2O_leaf reduced vpdl from 1.69 to 1.45 kPa for the

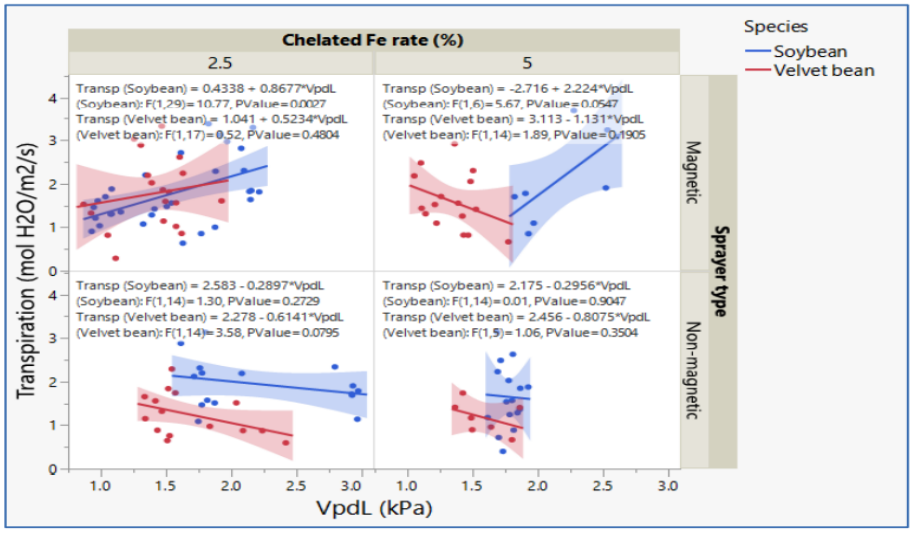

Figure 5: Linear regression for transpiration by vpdl for second water stress gas exchange test by species. Chelated Fe rate (upper x-axis), sprayer type (right y-axis), and species (legend).

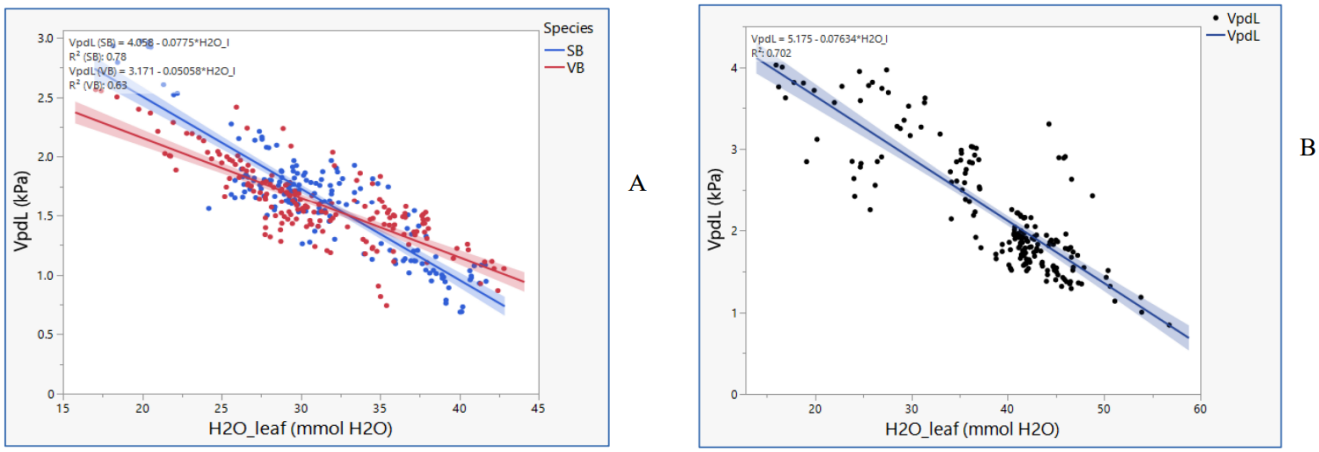

Figure 6: Linear regression between H2O_leaf and vpdl by species (legend) across this study's three gas exchange collection dates (**A**). Regression between H2O_leaf and vpdlfor Ramsey study [3] (**B**) for the low soil moisture irrigation treatment.

velvet bean plants in the second water stress test. The soybean plants experienced a loss in H2O__leaf, so there was no reduction in vpdl in the second water stress test. The predicted H2O_leaf parameter was used in the raw data regression to estimate the probable rise in the H2O_leaf parameter due to increased levels of BSW water in the optimal treatment.

The water vapor parameters in both studies were calculated using the software models built into the gas exchange instrument. The models that calculate vpdl use leaf temperature and vapor pressure parametersto estimate saturated vapor pressure (SVTleaf), which is used in another model to calculate vpdl (kPa). These models are based on a standard water vapor pressure over temperature algorithm. Many of the water vapor parameters calculated by the LICOR gas exchange models are based on the primary leaf temperature variable. In other words, higher leaf temperatures will translate into higher values for the water vapor parameters calculated by the software models. The water vapor pressure over temperature algorithm for BSW water is shifted to higher temperatures than the water vapor pressure over temperature algorithm for tap water. Until a water vapor and temperature algorithm for BSW water is formalized the water vapor parameters calculated by the instrument software are the most reliable estimates. The water vapor pressure over temperature algorithms become relevant when comparing the predicted values for vpdl for the optimal treatment in Table **11** in the Ramsey study [3]. The predicted vpdl for the optimal treatment was 2.99 kPa for the low soil moisture target, which is significantly over the generally accepted vpdl threshold of 1.25 kPa when partial stomatal closure is initiated.

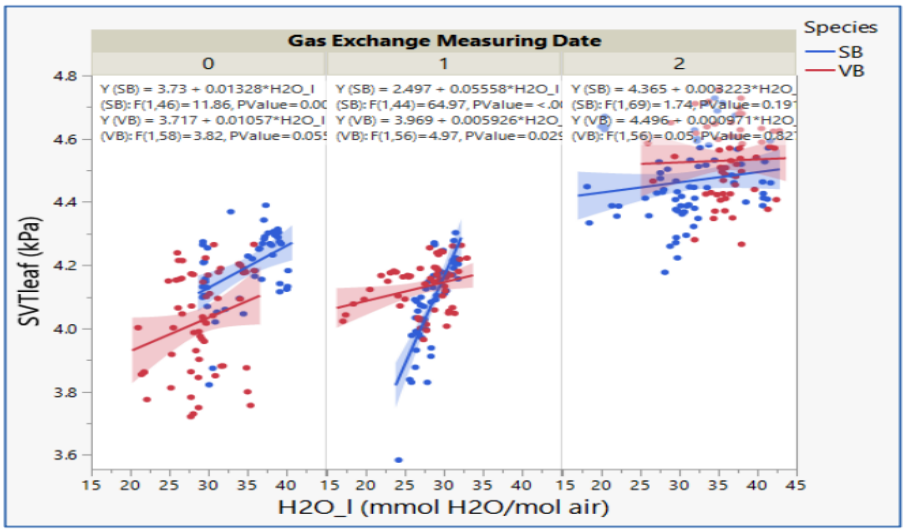

Figure 7: Linear regression between SVTleaf over H2O_leaf by species (legend) by gas exchange measurement date (upper x-axis).

There is a positive linear regression between saturated vapor pressure (SVTleaf) and mole fraction of water vapor (H2O_leaf) in the intercellular airspaces for the baseline measurements (Figure **7** left graph). This positive relationship shows that water vapor pressure (kPa) increases with increasing molar fraction of water vapor (H2O_leaf) inside leaves for non-water stressed plants and plants under moderate water stress under ambient light. This positive relationship became non-significant or uncorrelated for the second water stress treatment (Figure **7** right graph) when the plants were under the HID MH lamps. This change in the relationship between these two water vapor parameters between the baseline and second water stress treatment is unexplainable. This anomaly between SVT leaf and H2O_leaf for water-stressed plants should be investigated further due to the implications on plant defense activities. The interconnectivity between transpiration, stomatal conductance, SVTleaf, and H2O_leaf may shift to an unexpected set of connective relationships for plants under water stress.

Gas exchange parameters were predicted using repeated measures (REML) models for seven gas exchange parameters(Tables **4-5**). The tables were separated by species, and the gas exchange parameters were reported for the three measurement dates to make a longitudinal or before-and-after comparison of treatment effects.

A comparison of the soybean table (Table **4**) between the baseline and second water stress parameters for the magnetic sprayer with 5% chelated iron foliage treatment shows that soil moisture was reduced by 48%. The same comparison between the baseline and the magnetic sprayer with 5% chelated iron shows that transpiration (43%), SVTleaf (6%), and Ci/Ca (20%) increased after the foliage treatment and after moving the plants into the second bay with the HID MH lighting system (Table **4**). However, the same comparison also shows that photosynthesis (20%), stomatal conductance (4%), and H2O-leaf (12%) decreased after the foliage treatment and after moving the plants under the HID MH lamps (Table **4**). In other words, photosynthesis, stomatal conductance, and H2O-leaf decreased by 20, 4, and 12% after soil moisture decreased by 48% when comparingthe baseline parameters with the same parameters after the foliage treatments. The soybean results show that saturated vapor pressure inside the leaf (SVTleaf in units of kPa) increased by 6%, but the water vapor mole fraction (H2O_leaf in units of mol H_2O) inside the leaf decreased by 12%. The results of these water vapor parameters are inconsistent, which is difficult to explain as both parameters measure the same water vapor conditions within the intercellular airspaces of a leaf. They should increase or decrease in parallel with each other, as shown in Figure **7** for the baseline treatment (left graph). The dataset shows that the H2O_leaf data had higher values in the baseline measurements that could not be explained.

A comparison of the velvet bean table (Table **5**) between the baseline and second water stress parameters for the magnetic sprayer with 5% chelated iron foliage treatment shows that soil moisture was reduced by 37%. The same comparison between the baseline and the magnetic sprayer with 5% chelated

Table 4: Predicted Gas Exchange Parameters Based on the JMP REML Model for Baseline, First, and Second Gas Exchange Measurements for Water-Stressed soybean Plants. Gas Exchange Parameters are only Listed for Chelated Iron Applied at 5%

Gas Exchange Parameters	Baseline Values	First Water Stress Values		Second Water Stress Values	
		Magnetic	Non-magnetic	Magnetic	Non-magnetic
Photosynthesis(umol $CO_2/m^2/s$)	6.51	2.14	2.27	5.20	5.32
Transpiration(mol $H_2O/m^2/s$)	1.35	0.64	0.56	1.82*	1.24
Stomatal Cond.mol/m^2/s)	0.06	0.014	0.025	0.088*	0.086
Vpdl (kPa)	1.19	1.58	2.21	1.83*	1.85*
Leaf temp. (C)	29.9	29.2	29.1	30.6*	30.6*
Ci/Ca	0.59	0.1	0.81	0.77	0.63
SVTleaf (kPa)	4.20	4.09	4.01	4.45*	4.49*
H2O_l (mmol H_2O/mol air)	34.8	25.1	28.9	30.7*	30.3
Soil moisture ((% v/v)	0.40	0.18	0.18	0.21*	0.27*

[a]vpdl = vapor pressure deficit for leaf, Ci/Ca = ratio of internal CO_2 to atmosphere CO_2, SVTleaf = saturated vapor pressure in leaf, H2O_l = water vapor concentration inside leaf. Second, water stress parameters with * were significantly different from the baseline parameters.

Table 5: Predicted Gas Exchange Parameters Based on the JMP REML Model for Baseline, First, and Second Gas Exchange Measurements for Water-Stressed velvet Bean Plants. Gas Exchange Parameters are only listed for Chelated Iron Applied at 5%

Gas Exchange Parameters	Baseline Values	First Water Stress		Second Water Stress	
		Magnetic	Non-magnetic	Magnetic	Non-magnetic
Photosynthesis(umol $CO_2/m^2/s$)	5.55	2.56	2.68	3.46	3.56
Transpiration(mol $H_2O/m^2/s$)	0.97	0.28	0.21	1.61*	1.03*
Stomatal Cond.(mol/m^2/s)	0.068	0.021	0.002	0.10*	0.06
Vpdl (kPa)	1.47	2.21	1.57	1.71	1.48
Leaf temp. (C)	29.1	29.6	29.7	30.9*	31.2*
Ci/Ca	0.57	0.03	0.74	0.81	0.73
SVTleaf (kPa)	4.02	4.14	4.06	4.51*	4.56*
H2O_l (mmol H_2O/mol air)	30.01	23.2	30.7	33.7*	37.0*
Soil moisture ((% v/v)	0.36	0.12	0.20	0.22*	0.21*

[a]vpdl = vapor pressure deficit for leaf, Ci/Ca = ratio of internal CO_2 to atmosphere CO_2, SVTleaf = saturated vapor pressure in leaf, H2O_l = water vapor concentration inside leaf. Second water stress parameters with * were significantly different from the baseline parameters.

iron shows that stomatal conductance (64%), transpiration (44%), SVTleaf (12%), H2O-leaf (16%), and Ci/Ca (33%) increased after the foliage treatment and after moving the plants under HID MH lighting system (Table **5**). However, the same comparison only shows that photosynthesis (37%)decreased after the foliage treatment and after moving the plants under the HID MH lamps (Table **5**). In other words, only photosynthesis decreased by 37% after soil moisture decreased by 37% compared to the baseline parameters and the same set of parameters after the foliage and HID MH lamp treatment for velvet bean plants. The reduction in photosynthesis most likely reflects increased carbon assimilation efficiency instead of a reduction in overall biomass production. The study was not designed to evaluate improvements in photosynthetic efficiency. Therefore, no conclusions for improved efficiency can be drawn from these results. The REML model shows that SVTleaf and H2O_leaf increase in parallel with each other for the magnetized sprayer and chelated iron (5% Fe) in the second water stress measurements for velvet bean plants. This direct relationship aligns with velvet beans' baseline results (Figure **7**, left graph).

Instantaneous Water Use Efficiency (WUE), a non-linear parameter, was transformedusing a reciprocal equation that allows linear regression with other linear

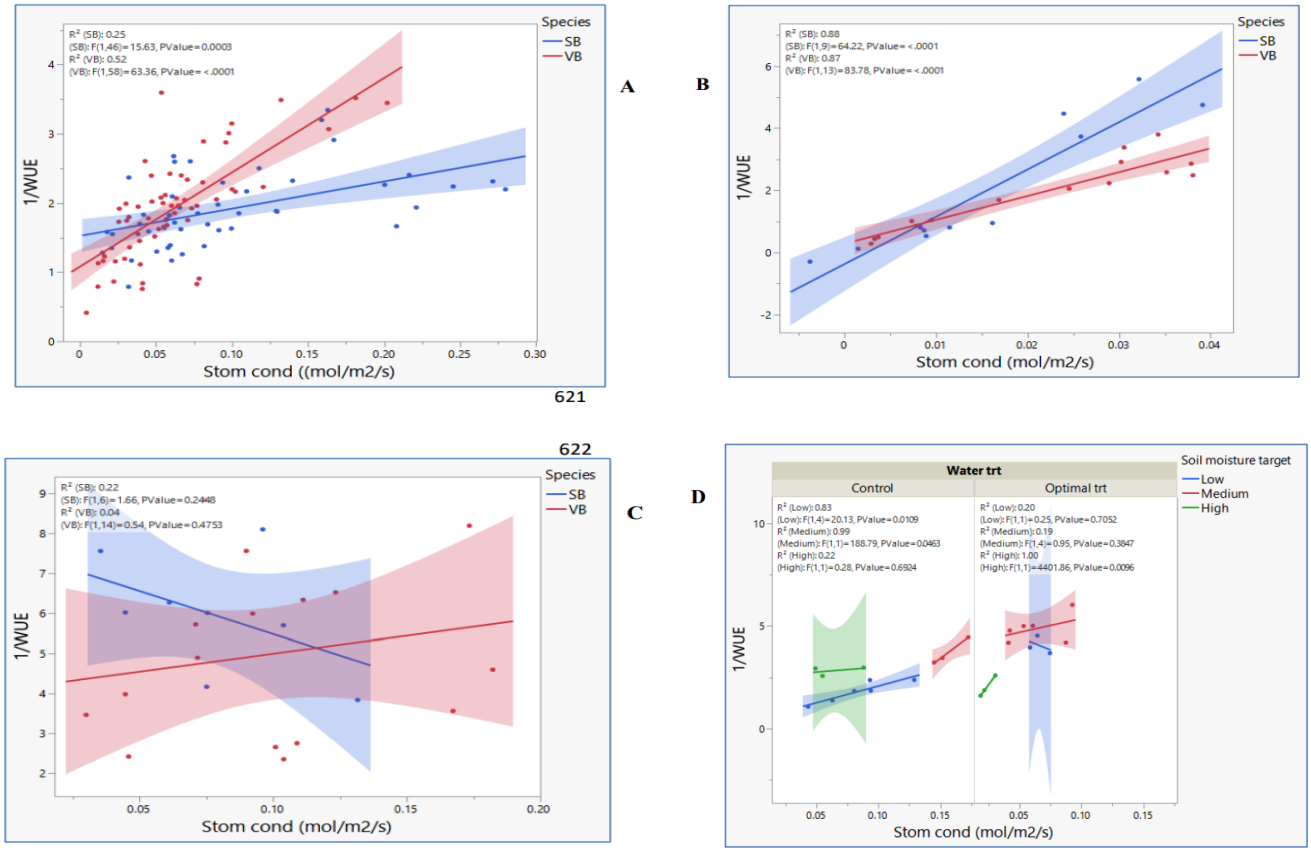

Figure 8: Linear regression of reciprocal of Water Use Efficiency (1/WUE) over stomatal conductance for baseline (**A**), first (**B**), and second (**C**) water stress data collection dates. Graph **D** was added to compare the results between this study and the Ramsey [3] study. Graph **D** also shows the 1/WUE over stomatal conductance linear regression for the Ramsey [3] study, which includes all three soil moisture levels.

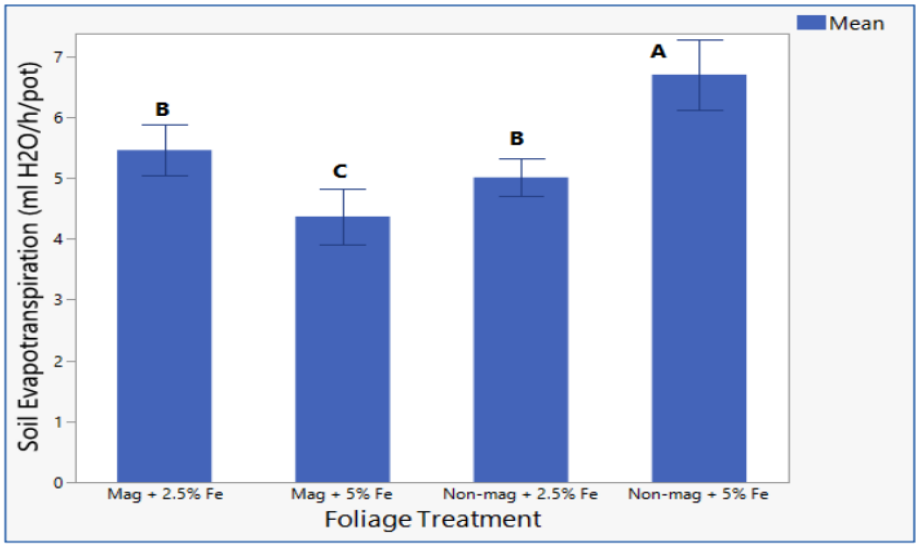

Figure 9: Estimated soil evapotranspiration rate for the foliage treatments during the second water stress treatment.Evapotranspiration rates were estimated as water losses on an hourly basis (y-axis in ml H_2O/h/pot).

parameters. The reciprocal of the WUE (1/WUE) was regressed over stomatal conductance for both this study and the Ramsey study [3] (Figure **8**). The before or baseline graph (Figure **8** graph A) shows a positive linear relationship between 1/WUE and stomatal conductance, with significant *p*-values reported for both

species. In contrast, there is no relationship between 1/WUE and stomatal conductance (Figure **8** graph C) for both species (*p*-values >0.05) for the foliage treatments during the second water stress treatment. In other words, instantaneous water use efficiency was unlinked from stomatal conductance for both species due to the effects of the study factors on gas exchange responses for plants under water stress.

he same regression test was run for the gas exchange responses in the Ramsey study [3]. The control and optimal treatments were combined into one graph (Figure **8** Graph D) for this study. The control treatment had a positive relationship between 1/WUE and stomatal conductance for the low and medium soil moisture treatments (*p*-values < 0.05) for velvet bean plants. However, this positive relationship reverted to no relationship between 1/WUE and stomatal conductance for the optimal treatment of low and medium soil moisture. The magnetized seed and structured water treatments unlinked instantaneous water use efficiency from stomatal conductance.

The foliage treatment with the magnetized sprayer and chelated Fe (5%) in the second bay with the HID MH lamp system had the lowest soil evapotranspiration rate (4.4 ml H_2O/h/pot) (Figure **9**). The soil evapotranspiration rate was calculated using the soil moisture data described in the Material and Method section.

The seeds were planted at different dates for each species, so the total number of days between planting and harvest for each species was used to estimate the daily growth rate. Also, the velvet bean plants' growth was diminished by a mite infestation near the end of the study. The study design did not include harvesting control plants to compare growth rates with untreated plants. The total number of days between seed planting and harvest was 157 and 136 days for soybean and velvet bean plants, respectively. The use of average growth rates is deceptive if the plants are very mature, as the exponential growth rates for annual plants are typically during the first two months. These two legume species are generally considered annuals, and the plants were well into senescence at harvest time, resulting in very low daily growth rates for both species.

4. DISCUSSION

This discussion section starts with a short review of the effects of infrared radiation on plant functions and water properties to support and add credibility to the results and conclusions reached in this study. Recent literature shows that electromagnetic energy in red, far red, and all infrared spectral bands increasesplants' water structure and BSW water content [2-6].As plants' BSW water levels increase, sap flow and transpiration dynamics are also enhanced [3, 7].

The effects of visible (red to far-red wavelengths) and infrared wavelengths (near, mid, and far IR) on hydrogen bond properties in liquid water were reviewed by Ramsey [4 -6}. On a free access website, Chaplin thoroughly reviews water properties and structure [27]. His review of hydrogen bonds in water explains how H-bond length and strength are related to water structure. He cites articles stating that thermal energy radiation of liquid water, such as infrared radiation, will expand the distance between water molecules. As expansion causes the water molecules to separate, the electron density distribution over the oxygen atom increases, promoting stronger hydrogen bonds that reform after the added energy dissipates and water cools again [27]. Areview article on hydrogen bonds by Tao *et al*. [28] states that there is a strong linear relationship between hydrogen bond strength and delocalization energy in molecules.His review also states that molecular dynamics simulation models show that increasing water temperature breaks weak electrostatic-based hydrogen bonds, and the number of strong hydrogen bonds increases during the reformation of water molecules [28]. As H-bond strength increases, water structure increases as H-bonded water self-assembles into a range of dimer to hexamer supramolecular clusters. The strongest H-bonds form hexamer water structures [28], the most common designs in biologically structured water [4-6].

Pollack's theory for BSW or Exclusion Zone (EZ) water explains the relationship between water structure and BSW properties on biological surfaces. Pollack *et al*. [7-14] and Hwang *et al*. [12] state that BSW water forms an EZ zone that covers all membrane and cell surfaces in plants and animals. The EZ zone is a liquid crystalline lattice of multi-layered, continuoussheets of hexagonal-ringed water molecules, including openings for aquaporins and ion channels in cell membranes [7-14]. Pollack published microscopic images of EZ zones on Nafion surfaces with a depth of up to 250 µm and had a peak light absorption of 270 nm [7]. He states that red, far red, near-infrared, and far infrared wavelengths increase the EZ zone on hydrophilic surfaces [7]. Also, Pollack states that water preferentially absorbs and increases in structure when

exposed to IR bands ranging from 3,000 to 15,000 nm or at the low end of the FIR band [7]. Sharma *et al*. [14] reconfirmed that strongly hydrophilic surfaces such asghee (clarified butter) and cellulose paper (Whatman filter paper) can produce EZ water in the liquid and solid state. Also, Pollack [7] published a crypto image of an xylem vessel infused with ink microspheres and taken with a transmission electron microscope (TEM). The TEM image clearly shows an EZ zone on both walls of the xylem, with the ink sphere excluded or repelled into the middle of the xylem vessel.

The BSW water review by Ramsey [4-6] refers to several research phrases that are often used as substitutes or synonyms for BSW water, such as membrane hydration water, vicinal water, interfacial water, bound water, non-freezing water, liquid crystalline, and EZ water. A review of water transport in woody plants by Siau [29] estimated the percentage of bound water in woody plant tissue. He found that bound water generally accounts for ~30% of the total water, expressed as water mass per dry wood mass. A plant water content study by Pissis [30] also states that bound water represents approximately 30% of the total water content of plants. A book by Skaar [31] states that the percentage of bound water in woody plants varies with plant water stress levels. A food processing study by Khan *et al*. [32] differentiated water in plant-based foods such as grain, fruits, and vegetables into three categories: free water (intercellular water), loosely bound water (LBW), and strongly bound water (SBW) as intracellular water. They state that plant-based food contains 6-15% free water, 80-92% LBW, and 1-6% SBW.

Recent research concludes that red light and IR energy bands positively affect plant health, yield, and cold and water stress tolerance. Huang *et al*. [33] studied the effects of red and yellow LED wavelengths on the drought tolerance of fava beans (*Vicia faba*). They found that the red and yellow LED lamps produced smaller leaves and higher relative water content (RWC) in the leaves. Affandi *et al*. [34] evaluated the effects of supplemental FR LED lamps on the cold tolerance of tomatoes. They found that adding FR lamps reduced weight loss, less pitting, less softening, and faster red color development in tomatoes. They also state the FR lamps improved the cold tolerance in tomatoes. Ouedraogo and Hubac [35] found that FR lamps increased drought tolerance in cotton. Li *et al*. [36] studied the effect of far infrared (FIR) lamps on tomatoes. They found that FIR increased photosynthesis by 44% and tomato yield by 21% compared to the control. Nemera *et al*. [37] studied the effects of red shade netting with 20% shading on Valencia oranges. They found that the red netting had reduced stem water potential under deficit irrigation (60% reduction), i.e., the xylem vessels were under less water stress than the control. They also tested the spectral transmission of the shade nets. They found that the red netting transmitted wavelengths within two bandsof 300 - 350 nm and > 600 nm, and the red netting had a higher orange yield. Zhang *et al*. [38] evaluated the effects of multi-spectral LED lamps and High-Pressure Sodium (HPS) lamps on cotton growth and gas exchange. They found that the LED lamps with the highest PAR intensity in the far red (FR) spectrum also produced the most leaves and had the highest biomass. Also, the LED lamp with the highest FR spectrum had the highest photosynthesis rates and longest palisade cells. This study reveals that PAR spectral qualities affect leaf morphology in terms of the length of palisade cells and the thickness and density of spongy mesophyll cells [38]. This study also shows a correlation between the adaptation of cellular structure in the leaves due to light spectral qualities and gas exchange rates.

Along with Pollack's theory on EZ water, he also postulated that EZ water causes water movement in tubes and micro-sized channels via his proposed hydronium ion ($H3O^+$) drive, or"proton drive theory"[7]. The widely accepted Cohesion-Tension theory used to explain sap flow in plants states that water is transported in xylem vessels under negative pressure potential created by leaf transpiration. His EZ water theory states that the EZ zone excludes all solutes and ions, including hydronium ions, that are repelled into the free water zone adjacent to the interfacial water zone. Pollack's proton drive theory states that the electrostatic charge properties of EZ water 'push" or repel water through the plant vascular system. To support this theory, Pollack published a crypto image of an xylem vessel infused with ink microspheres and taken with a transmission electron microscope (TEM) [7]. The TEM image clearly shows an EZ zone on both walls of the xylem, with the ink sphere excluded or repelled into the middle of the xylem vessel. Sharma *et al*. [14] also state that EZ water can form or self-assemble into a distinct zone on cellulose paper filter paper,i.e., cellulose has hydrophilicproperties that encourage the formation of EZ water zones.

The hydronium ion ($H3O^+$) drive or proton-drive theory relieson energy inputs such as infrared energy from sunlight or respiration to energize free water to self-

assemble into EZ zone or BSW water. As the EZ or BSW water zone increases, the hydronium ions (H_3O^+) concentration also increases, and the ions are expelled by the EZ zone and also at the capillary meniscus. In other words, plants use sunlight's red and infrared spectrum to generate and thicken the EZ or BSW water zone that coats the inside of the xylem vessels. The positive charges within the concentrated zone of expelled hydronium ions accumulate, and electrostatic forces start repeling the H_3O^+ ions up the xylem vessels. In essence, electrostatic forces cause the continuous generation of positive ions in sap to flow upwards against the pull of gravity, depending on the thermal energy inputs to generate the positive ions [7]. Although xylem vessels are dead cells, the lignin component in the xylem walls has a negative charge of -30 mV [39]. During cavitation, the negative charge of lignin attracts the positively charged hydronium ions, pulling the H_3O^+ ions up the xylem vessels. This same principle also forces water to move autonomously in horizontal inanimate tubes that can form EZ water.

A sap flux study by Vandegehuchte and Steppe [40] found that sap flux density measurements could be improved in European (*Fagus sylvatica*) and American (*Fagus grandifolia*) beech and Eucalyptus (*Eucalyptus caliginosa*) by correcting for thermal diffusivity parameters. They developed sap flow models that adjusted for the difference in thermal diffusivity between bound and unbound water, resulting in more accurate sap flux density estimates. Their study acknowledged that xylem vessels contained both bound and non-bound or free water. Also, they show that sap flow is a function of the water property differences between the two water types. A study by Fedorets *et al*. [41] found that infrared radiation of water resulted in self-organized, hexagonal-patterned, supramolecular lar water clusters. They also found that the infrared radiation stabilized the water clusters.

The HID MH lamps in the second water stress treatment emitted IR radiation in the NIR and FIR bands. Based on IR spectra reported by Krizek *et al*. [23], the HID MH lamps probably had an NIR to FIR intensity of 893 w/m^2 9 (4,108 µmol/m^2/s) and 225 µmol/m^2/s in the FIR band alone. The HID MH lamps were positioned about 1.2 m above the top of the plants. Thus, the plants were radiated with moderately intense visible light and IR radiation from the HID MH lamps.

Infrared and FR light also positively affect water structure in plant tissue and provide an energy source for sap flow in plants [42-44]. Boini [44] tested the effects of five different colored shade nets on apple trees. Their shade nets filtered light wavelengths from 400 to 700 nm (PAR wavelengths) up to 1,000 nm (near-infrared wavelengths). They found that the standard black netting with 18-21% shade reduction had a wavelength transmission range that peaked from 700 to 1,000 nm, i.e., most of the light was transmitted in the far red to near-infrared spectrum. The black netting had the highest average apple growth rates compared to the other four colored nets. Also, in 8 out of 10 sap flow and fruit measurement dates, the red or black shade netting increased sap flow the most, as well as increased apple fruit growth. These study findings show that shade netting with peak transmission in the red to NIR spectral range also resulted in the highest sap flow rates [44].

Lee *et al*. [45] compared far infrared (FIR) treated chicken compost with chemical fertilizer effects on maize growth. The compost was layered with sheets of composite material that inherently emitted far infrared radiation (4,000 to 1,400 nm) without electrical input. The sheets contain embedded resistance material sandwiched between hardened glass or vitrified ceramic. The layered sheets radiated infrared energy, altering the compost properties and enhancing maize yields. The FIR chicken compost treatment increased ear length and the average year yield by 24% compared to the chemical fertilizer treatment. Also, the 100 kernel weight increased 20% for the FIR chicken compost treatment. These findings agree with the study by Li *et al*. [36] that showed a 21% increase in tomato yield due to FIR foliage treatments. This first-of-its-kind compost treatment study using FIR-emitting composite ceramic materials holds much promise for altering compost and compost water properties.

Water-stressed plants defend against high water vapor gradients or vpdl levels by partially closing stomata and reducing transpiration rates to minimize excessive water vapor losses [46]. Transpiration is biphasic and starts with a linear relationship with vpdl, estimated from the difference between saturated vapor pressure in the air (SVTair) and relative humidity (RHair). As vpdl increases, a threshold is reached, initiating a decrease in stomatal conductance, and transpiration enters the second biphasic function with a plateau or reduction phase for plants under water stress. The interactions between transpiration, vapor pressure deficit, and stomatal conductance are included in a suite of plant defenses activated to reduce

photosynthetic and plant injury due to excessive water vapor losses. The multivariate results from this study parallel the multivariate findings in the study by Ramsey [3]. The two studies had significant pairwise correlations in the baseline results for the transpiration, stomatal conductance, SVTleaf, and SVTair correlations that mirrored each other. These baseline correlations became unlinked or uncorrelated after the foliage and the HID MH lamp treatments for the gas exchange measurements during the second water stress treatment.

The level of BSW water in plant tissue increased in this study and the Ramsey study [3] due to the different combinations of plant treatments. The increase in water vapor in the intercellular airspaces, based on increases in SVTleaf and H2O_leaf values, is evidence of increased BSW water levels in plant tissue. These increases in water vapor occurred despite the reduction of soil moisture levels down to 2% in the Ramsey study [3] and 21 % (v/v) in this study. As water vapor pressure (SVTleaf) or mole fraction of water vapor (H2O_leaf) increases within the intercellular airspaces in leaves, a concomitant reduction in vpdl also occurs. In other words, as water vapor pressure increases within the leaf, the vapor pressure differential between the leaf and air is reduced due to the inverse relationship between H2O_leaf and vpdl (Figure **6**). Also, SVTleaf has a positive relationship with H2O_leaf (Figure **7**) showing that both parameters increase in parallel as water vapor increases in the intercellular airspaces. Plants under water stress with a higher mole fraction of water vapor have a lower vapor pressure deficit, are less stressed, and maintain healthier gas exchange responses (Figure **6** and Tables **4-5**).

Despite the numerous differences between this study and the Ramsey study [3] design and treatments, up to nine interconnected gas exchange responses were disassociated or unlinked and correlated with plant defense activities in the baseline responses. The multivariate results from this study reveal that transpiration was not correlated with SVTair or RHair for the magnetized spray and chelated iron (5% Fe) treatment for both legumes for the second water stress treatment (Tables **2-3**). The correlation *p*-values for soybean plants for transpiration and SVTair (*p-v*alue = 0.1993) show no relationship between transpiration and SVTair. For velvet beans, there is no relationship between transpiration and SVTair (*p-v*alue = 0.2401), and for transpiration with RHair (*p-v*alue = 0.7682). These findings mirror the Ramsey study results above [3] (Tables **2-3**). The study by Ramsey [3] revealed that transpiration was not correlated with SVTair (*p-v*alue = 0.7581) or RHair (*p-v*alue = 0.5962) for the magnetized seed and structured water treatment.

The linear regressions between transpiration and vpdl (Figure **3-5**) for both studies show disconnection or unlinking between the baseline or control treatment and the water stress treatments. The negative relationship between transpiration and vpdl for soybean and velvet bean for the baseline (Figure **3**) treatments becomes non-significant for both species in the second water stress treatment for the magnetized sprayer with chelated iron (5%) (Figure **5** upper right graph). These regression findings agree with the multivariate findings. Also, the loss in regression relationship and correlation analysis implies that these connected gas exchange parameters became disconnected and unlinked with each other after testing the effects of the study factors in the analysis.

Another disconnection or unlinking occurred in the relationship between instantaneous water use efficiency and stomatal conductance when comparing the baseline with the second water stress treatment. The gas exchange responses between 1/WUE and stomatal conductance were also analyzed using a linear regression test (Figure **8**). The reciprocal of WUE or 1/WUE allows linear analysis of WUE. However, an increase in 1/WUE actually decreases water use efficiency (WUE). For example, the baseline graphs in Figure **8**. show an increase in 1/WUE, which equates to a decrease in WUE as stomatal conductance increases. The positive relationship is counterintuitive to the negative linear relationship between WUE and stomatal conductance. The regression tests for both studies show that instantaneous water use efficiency (WUE) had no relationship with stomatal conductance for the optimal foliage, seed, and water treatments (Figure **8** graphs C -D). The interconnectivity for regulatory defense activities for these two gas exchange responses was unlinked and became non-correlated.

Soil evapotranspiration is the sum of water losses from soil evaporation and plant transpiration rates. This reduction in soil moisture losses occurred simultaneously with an increase in transpiration of 43 and 44% for soybean and velvet bean plants, respectively, for the same foliage treatment. The simultaneous water saving in soil moisture with increased transpiration indicates increased metabolic efficiency and or increased water use efficiency (WUE)

for the magnetized sprayer and chelated Fe (5%) foliage treatment under the HID MH lamps (Figure **8**). In the Ramsey study [3], transpiration increased by 226%, soil moisture decreased to 2% (v/v). In comparison, whole plant WUE increased by 87% for the optimal treatment under the low soil moisture treatment.

The first article of this study [1] reported on the effects of the study factors on gas exchange responses to two water stress treatments. The latest analyses for this study closely mirror the results of the study by Ramsey [3]. It is important to note that this study was conducted eight years earlier than the Ramsey study [3]. Also, the initial study design and treatments in this study were different, unrelated, or connected to the study design for the Ramsey study [3]. In other words, these two completely different studies somehow concluded with remarkably comparable results when using similar data analysis tests. Also, both study analyses show that the study factors maintained BSW water levels in the sap and plant tissue. Maintaining BSW water levels resulted in deactivating a suite of interconnected regulatory gas exchange parameters and plant defense activities. Deactivation of this suite of regulatory plant defenses reduced stress levels, conserved water resources, enhanced drought tolerance, increased metabolic and water use efficiency, and minimized growth losses in water-stressed plants.

These two studies' findings also open up questions involving the basic tenets of the Cohesion-Tension theory used to explain sap flow in plants. This theory is based on the combination of the strength of hydrogen bonds in water (water cohesion) with the negative pressure potential in the xylem (water tension), which explains plant sap flow. However, these studies suggest that transpiration, stomatal conductance, and several water vapor parameters can be unlinked or disassociated in water-stressed plants. If unlinking a suite of regulatory gas exchange responses with transpiration is possible, then the Cohesion-Tension theory that explains sap flow becomes questionable. Negative pressure potential in water columns in the xylem is ultimately a function of transpiration rates as water vapor exits the stomata. The unlinking of transpiration with vpdl implies that the negative pressure potential may fluctuate widely enough to create insignificant or inconsistent pressure gradients to drive sap flow reliably. Perhaps the Cohesion-Tension theory should be expanded to include Electrostatic forces as well, i.e., a revised Cohesion-Tension-Electrostatic (CTE) theory contains all the underlying mechanisms involved in sap flow.

Recent research uncovers the effects of near (NIR) and short wave (SWIR) infrared wavelengths on plant physiology, morphology, growth, and yield [26, 47- 49]. The interactions between IR radiation and plant foliage and tissue are complex [26, 47]. Foliage and green plant tissue reflect, transmit, or absorb visible and non-visible wavelengths. NIR wavelengths (780 to 1,400 nm) are non-visible and occur just after far-red visible wavelengths. They are the shortest IR spectral band, which can rapidly be absorbed by water tissue, raising leaf temperatures quickly. Plant foliage typically absorbs less than 10% NIR to prevent increasing foliage temperature and avoid excessive leaf injury. The mid-IR or SWIR spectral IR band (1,400 to 3,000 nm) is also absorbed by water in plant tissue and cellulose at 1,800 nm [26]. As cellulose absorbs SWIR energy, Pollack postulated that this absorbed energy is used to maintain and/or increase EZ zones in xylem vessels [7].The far-red IR spectral band (3,000 to 100,000 nm) is sometimes called the thermal reflective band. Some of the NIR and SWIR radiation absorbed by plants is re-emitted back out of the foliage at longer FIR wavelengths that thermal cameras can detect. The tradeoff of longer wavelengths for FIR radiation is lower water absorption rates, higher penetration into woody tissue, and deeper penetration into dense foliage [26, 47]. Each IR spectral band has advantages and disadvantages concerning sap flow, water structure, and water content in plant tissue, depending on the intensity and duration of IR radiation.

Chlorophyll absorbs visible light in the PAR spectral band (400-700 nm) and converts a percentage of this visible light into fluorescence re-emitted from the leaf. The estimated peak in chlorophyll fluorescence is in the NIR spectrum (~ 750 nm) [50]. This NIR peak also coincides with one of five major water absorption bands in the NIR spectrum at 760, 970, 1,190, 1,450, and 1,940 nm, with a weaker absorption band at 845 nm [51]. Although the adaxial surface of leaves absorbs less than 10% NIR energy, chlorophyll fluorescence has peak NIR emittance at 750 nm that is readily absorbed by water in foliage with preferential absorption at 760 nm. In summary, excess PAR energy is partially converted into NIR wavelengths absorbed by water inside leaves, increasing EZ or BSW water levels in plant tissue.

The multifaceted interactions between visible and IR light, foliage optics, and canopy properties are very

complex. Foliage optics account for the reflectance, absorption, and transmission of energy, which are functions of light and leaf properties. Canopy properties and dynamics exponentially increase the complexity of the interactions between light and infrared wavelengths and leaf optics. For example, canopy properties and dynamics affect the penetration of light and infrared radiation, light intensity, and quality dynamics, reflectance and re-absorbance rates, light scattering, chlorophyll fluorescence, and abaxial absorption, to name a few of these interactions. DeLucia *et al*. [52] evaluated the effects of light scattering inside leaves or intercellular reflectance on photosynthesis in shaded leaves. They found a 1.97-fold increase in photosynthesis due to intercellular light scattering in shade leaves. The interactions between indirect light and IR sources, foliage optics, and canopy properties have yet to be fully explored. For example, visible light, or PAR wavelengths, are readily converted into infrared wavelengths in the form of fluorescence when chlorophyll receives light above its saturation capacity. As mentioned above, chlorophyll fluorescence and intercellular light scattering may increase water absorption of NIR wavelengths within each leaf. Also, chlorophyll fluorescence may be reflected outside a leaf and be absorbed by the underside or abaxial surface of leaves above it. Abaxial leaf absorption of NIR occurs in the spongy mesophyll cells with high liquid water content, with the likelihood of increasing water structure [49, 52 - 54]. Mesophyll cells also have chlorophyll and can contribute to photosynthesis along with their primary function of releasing water vapor into the intercellular airspaces.

Several studies have shown that abaxial gas exchange ratesdo not interfere with adaxial gas exchange rates. Nishio *et al*. [55] found that the chlorophyll in spongy mesophyll cells in spinach (*Spinacia oleracea L.*) leaves increased total leaf photosynthesis by 40%. Driscoll *et al*. [56] found that abaxial photosynthesis was three to four-fold higher than adaxial photosynthesis. Also, Wall *et al*. [57] found that adaxial photosynthesis contributed about 50% to the total leaf photosynthesis rates without restricting CO2 uptake on either side of maize leaves. Zhang *et al*. [58] simulated alternating adaxial and adaxial radiation effects on leaves. They concluded that a bifacial leaf had higher photosynthetic rates than two “sun-leaf-like” leaves. These studies suggest that under-canopyradiation in greenhouses with LED lamps that emit low-intensity PAR and IR wavelengths could increase overall carbon assimilation rates. Under-canopy radiation with such LED lamps using higher radiation intensities may improve total photosynthesis in species with sufficient stomata numbers without interfering with CO_2consumption rates on either leaf surface.

Basic research is needed on the interactions between PAR and IR radiation on plant physiology and plant-water dynamics. Basic research is also needed on the primary effects of intensity and duration of IR radiation for each of the three bands (NIR, SWIR, and FIR) on plant physiology, morphology, and growth. Further research should be conducted on well water and water-stressed plants using supplemental LED IR lamps. Research is needed to determine the interactions between above-canopy and below-canopy lighting systems using LED lamps with PAR and IR wavelengths on gas exchange responses and growth. Also, research is necessary for SWIR and NIR radiation on abaxial leaf surfaces to determine the tradeoff threshold between increasing BSW water levels and raising leaf temperature above injury levels.

Applied research is needed to evaluate the cost-effectiveness of PAR and IR reflective fabric between crop rows to boost under-canopy radiation levels. Field research is needed to evaluate whether IR-enhancing stem collars or IR-enhancing netting on orchard crops is cost-effective. Also, could IR-emitting ceramic materials be used to line hoses to increase the structure of irrigation water? It may also be possible to mimic the cellulose and lignin composition of xylem vessels inside the hoses of the main and secondary drip irrigation lines. The study by Sharma *et al*. [14] found that cellulose fiber (Whatman filter paper) can produce EZ water on its surface. Cellulose paper filters withsolar-powered NIR lamps radiating the water-filled filters could be added at intervals along the irrigation lines. This irrigation hose design mimics xylem vessels composed of cellulose that absorb IR radiation to increase EZ water levels.

The findings from this study and the Ramsey study [3] show that the plant treatments improved resilience or drought tolerance in water-stressedlegumes. However, many greenhouse food production systems and other agricultural food systems are grown under well-watered conditions. Thus, it is important to distinguish between improving plant resilience for plants under abiotic stress and improving overall health and crop yields for crops grown under well-watered conditions. Several studies in the infrared review section reveal that crops not grown under water stress conditions and exposed to infrared radiation also improved crop yields [42 - 45].

Most food and plant production facilities would benefit from supplementing PAR LED lamps with SWIR and FIR LED lamps to increase crop yields, even for well-watered plants.

REFERENCES

[1] Ramsey C. Effects of Magnetized, Chelated Iron Foliage Treatments on Foliar Physiology, Plant Growth and Drought Tolerance for Two Legume Species. Global Journal of Agricultural Innovation, Research & Development 2021; 8: 66-86. https://doi.org/10.15377/2409-9813.2021.08.5

[2] Ramsey CL. Application of a structured water generator for crop irrigation: Structured water, drought tolerance, and alteration of plant defense mechanisms to abiotic stressors. J Basic Appl Sci 2021; 17: 127-52. Abstract: A greenhouse study was conducted to enhance drought tolerance in velvet bean plants. https://doi.org/10.29169/1927-5129.2021.17.14

[3] Ramsey CL. Magnetized Seeds and Structured Water: Effects on Resilience of Velvet Bean Seedlings (Mucuna pruriens) under Deficit Irrigation. Journal of Basic & Applied Sciences 2023; 19: 249-70. https://doi.org/10.29169/1927-5129.2023.19.19

[4] Ramsey CL. Biologically Structured Water (BSW)-A Review (Part 1): Structured Water (SW) Properties, BSW and Redox Biology, BSW and Bioenergetics. Journal of Basic & Applied Sciences 2023; 19: 174-201. https://doi.org/10.29169/1927-5129.2023.19.15

[5] Ramsey CL. Biologically Structured Water (BSW)-A Review (Part 2): Redoxbiology, SW Water and Plants, SW Drinking Water Types, BSW Water and Aging, BSW Water and Immunity. Journal of Basic & Applied Sciences 2023; 19: 202-229. https://doi.org/10.29169/1927-5129.2023.19.17

[6] Ramsey CL. Biologically Structured Water (BSW)-A Review (Part 3): Structured Water (SW) Generation, BSW Water, Bioenergetics, Consciousness and Coherence. Journal of Basic & Applied Sciences 2023; 19: 230-48. https://doi.org/10.29169/1927-5129.2023.19.18

[7] Pollack GH. The Fourth Phase of Water. Beyond Solid, Liquid, and Vapor. Ebner and Sons Publishers: Seattle, WA, USA 2013.

[8] Pollack GH. 11 Why Biological Water Differs from H2O and Acts Like. Bioelectromagnetic and Subtle Energy Medicine 2014; 105.

[9] Pollack GH Cell electrical properties: reconsidering the origin of the electrical potential Cell Biol Int 2015; 39(3): 237-342. ISSN 1065-6995 doi: 10.1002/cbin.10382. https://doi.org/10.1002/cbin.10382

[10] Pollack GH, Figueroa X, Zhao Q. Molecules, water, and radiant energy: new clues for the origin of life International Journal of Molecular Sciences 2009; 10(4): 1419-1429. https://doi.org/10.3390/ijms10041419

[11] Pollack GH Water, energy and life: fresh views from the water's edge International journal of design & nature and ecodynamics: a transdisciplinary journal relating to nature, science and the humanities 2010; 5(1): 27. https://doi.org/10.2495/DNE-V5-N1-27-29

[12] Hwang SG, Hong JK, Sharma A, Pollack GH, Bahng G. Exclusion zone and heterogeneous water structure at ambient temperature PLoS One 2018; 13(4). https://doi.org/10.1371/journal.pone.0195057

[13] Zheng JM, Pollack GH. Long-range forces extending from polymer-gel surfaces. Physical Review E 2003; 68(3): 031408. https://doi.org/10.1103/PhysRevE.68.031408

[14] Sharma A, Pollack GH. Healthy fats and exclusion-zone size. Food Chemistry 2020; 316: 126305. https://doi.org/10.1016/j.foodchem.2020.126305

[15] Whitewoods CD. Riddled with holes: Understanding air space formation in plant leaves. PLoS Biology 2021; 19(12): e3001475. https://doi.org/10.1371/journal.pbio.3001475

[16] Yong JW, Wong SC, Farquhar GD. Stomatal responses to changes in vapour pressure difference between leaf and air. Plant, Cell & Environment 1997; 20(10): 1213-6. https://doi.org/10.1046/j.1365-3040.1997.d01-27.x

[17] Conaty WC, Mahan JR, Neilsen JE, Constable GA. Vapor pressure deficit aids the interpretation of cotton canopy temperature response to water deficit. Functional Plant Biology 2014; 41(5): 535-46. https://doi.org/10.1071/FP13223

[18] Rockwell FE, Holbrook NM, Jain P, Huber AE, Sen S, Stroock AD. Extreme undersaturation in the intercellular airspace of leaves: a failure of Gaastra or Ohm? Annals of Botany 2022; 130(3): 301-16. https://doi.org/10.1093/aob/mcac094

[19] Buckley TN, Sack L. The humidity inside leaves and why you should care: implications of unsaturation of leaf intercellular airspaces. American Journal of Botany; 106(5): 618. https://doi.org/10.1002/ajb2.1282

[20] Pro Max 600 lamp spectral output. https://allgreenhydroponics.com/products/pro-max-grow-max600-full-spectrum-led-grow-light.

[21] Metal Halide lamp spectral output. https://www.globalgarden.co/products/hid-grow-lights/blv-horturion-mh-1000-watt-el-de-5-5k/

[22] Zeiss metal halide lamp website. https://zeiss-campus.magnet.fsu.edu/articles/lightsources/metalhalide.html.

[23] Krizek DT, Mirecki RM, Britz SJ, Harris WG, Thimijan RW. Spectral properties of microwave-powered sulfur lamps in comparison to sunlight and high pressure sodium/metal halide lamps.

[24] Supplemental greenhouse lighting. https://www.greenhouse-management.com/greenhouse_management/light_lighting_control_greenhouses/supplemental_greenhouse_lighting.htm

[25] Wein's law. https://www.omnicalculator.com/physics/wiens-law

[26] Ustin SL, Jacquemoud S. How the optical properties of leaves modify the absorption and scattering of energy and enhance leaf functionality. Remote Sensing of Plant Biodiversity 2020; 349-84. https://doi.org/10.1007/978-3-030-33157-3_14

[27] Chaplin water property and structure website. https://water.lsbu.ac.uk/water/water_hydrogen_bonding.html#e

[28] Tao Y, Zou W, Jia J, Li W, Cremer D. Different ways of hydrogen bonding in water-why does warm water freeze faster than cold water? Journal of Chemical Theory and Computation 2017; 13(1): 55-76. https://doi.org/10.1021/acs.jctc.6b00735

[29] Siau JF. Transport processes in wood. Springer Science & Business Media 2012.

[30] Pissis P, Angnostopoulou-Konsta A, Apekis L. A dielectric study of the state of water in plant stems. Journal of Experimental Botany 1987; 38(9): 1528-40. https://doi.org/10.1093/jxb/38.9.1528

[31] Skaar C. Wood-water relations. Springer Science & Business Media 2012.

[32] Khan MI, Wellard RM, Nagy SA, Joardder MU, Karim MA. Investigation of bound and free water in plant-based food material using NMR T2 relaxometry. Innovative Food Science & Emerging Technologies 2016; 38: 252-61. https://doi.org/10.1016/j.ifset.2016.10.015

[33] Huang L, Xiao Y, Ran J, Wei L, Li Z, Li Y, Zhang X, Liao L, Wang D, Zhao X, Xiao Q. Drought tolerance of fava bean (Vicia faba L.) can be improved by specific LED light wavelengths. Photosynthetica 2020; 58(4). https://doi.org/10.32615/ps.2020.052

[34] Affandi FY, Verdonk JC, Ouzounis T, Ji Y, Woltering EJ, Schouten RE. Far-red light during cultivation induces postharvest cold tolerance in tomato fruit. Postharvest Biology and Technology 2020; 159: 111019. https://doi.org/10.1016/j.postharvbio.2019.111019

[35] Ouedraogo M, Hubac C. Effect of far red light on drought resistance of cotton. Plant and Cell Physiology 1982; 23(7): 1297-303. https://doi.org/10.1093/oxfordjournals.pcp.a076474

[36] Li Y, Wu Z, Zhou R, Liu X, Hou X, Han M, Luo G, Zhou H, Jiang F. Improving tomato yield, quality and antioxidant capacity in greenhouse by far-infrared radiation. Plant Stress 2023; 10: 100274. https://doi.org/10.1016/j.stress.2023.100274

[37] Nemera DB, Dovjik I, Florentin A, Shahak Y, Charuvi D, Cohen S, Sadka A. Sparse-shading red net improves water relations in Valencia orange trees. Agricultural Water Management 2023; 289: 108533. https://doi.org/10.1016/j.agwat.2023.108533

[38] Zhang Y, Liao B, Li F, Eneji AE, Du M, Tian X. Growth, leaf anatomy, and photosynthesis of cotton (Gossypium hirsutum L.) seedlings in response to four light-emitting diodes and high pressure sodium lamp. Journal of Cotton Research 2024; 7(1): 8. https://doi.org/10.1186/s42397-024-00175-0

[39] Siddiqui L, Bag J, Mittal D, Leekha A, Mishra H, Mishra M, Verma AK, Mishra PK, Ekielski A, Iqbal Z, Talegaonkar S. Assessing the potential of lignin nanoparticles as drug carrier: Synthesis, cytotoxicity and genotoxicity studies. International Journal of Biological Macromolecules 2020; 152: 786-802. https://doi.org/10.1016/j.ijbiomac.2020.02.311

[40] Vandegehuchte MW, Steppe K. Improving sap flux density measurements by correctly determining thermal diffusivity, differentiating between bound and unbound water. Tree Physiology 2012; 32(7): 930-42. https://doi.org/10.1093/treephys/tps034

[41] Fedorets AA, Frenkel M, Bormashenko E, Nosonovsky M. Small levitating ordered droplet clusters: Stability, symmetry, and Voronoi entropy. The Journal of Physical Chemistry Letters 2017; 8(22): 5599-602. https://doi.org/10.1021/acs.jpclett.7b02657

[42] Meena RK, Vashisth AN. Effect of microenvironment under different colour shade nets on biophysical parameters and radiation use efficiency in spinach (Spinacia oleracea L.). Journal of Agricultural Physics 2014; 14(2): 181-8.

[43] Meena R, Vashisth A, Singh A, Singh B, Manjaih KM. Microenvironment study under different colour shade nets and its effects on biophysical parameters in spinach (Spinacia oleracea). J Agric Meteorol 2015; 16(1): 11-7.

[44] Boini A. Studies on apple physiology by managing light quality with photoselective nets. Doctoral dissertation, U. Bologna 2019.

[45] Lee MH, Chao YY. The Influence of Far-Infrared Materials Added to Compost on the Yield of Maize.

[46] Grossiord C, Buckley TN, Cernusak LA, Novick KA, Poulter B, Siegwolf R, Sperry JS, McDowell NG, Plant Responses to Rising Vapor Pressure Deficit. New Phytologist 2020 226: 1550–1566. https://doi.org/10.1111/nph.16485

[47] Jacquemoud S, Ustin SL. Modeling leaf optical properties. Photobiological Sciences Online 2008; 736: 737.

[48] Karabourniotis G, Liakopoulos G, Bresta P, Nikolopoulos D. The optical properties of leaf structural elements and their contribution to photosynthetic performance and photoprotection. Plants 2021; 10(07): 1455. https://doi.org/10.3390/plants10071455

[49] Cavaco AM, Utkin AB, Marques da Silva J, Guerra R. Making sense of light: The use of optical spectroscopy techniques in plant sciences and agriculture. Applied Sciences 2022; 12(3): 997. https://doi.org/10.3390/app12030997

[50] van der Tol C, Vilfan N, Dauwe D, Cendrero-Mateo MP, Yang P. The scattering and re-absorption of red and near-infrared chlorophyll fluorescence in the models Fluspect and SCOPE. Remote sensing of environment 2019; 232: 111292. https://doi.org/10.1016/j.rse.2019.111292

[51] Curcio JA, Petty CC. The near infrared absorption spectrum of liquid water. JOSA 1951; 41(5): 302-4. https://doi.org/10.1364/JOSA.41.000302

[52] DeLucia EH, Nelson K, Vogelmann TC, Smith WK. Contribution of intercellular reflectance to photosynthesis in shade leaves. Plant, Cell & Environment 1996; 19(2): 159-70. https://doi.org/10.1111/j.1365-3040.1996.tb00237.x

[53] Paradiso R, De Visser PH, Arena C, Marcelis LF. Light response of photosynthesis and stomatal conductance of rose leaves in the canopy profile: the effect of lighting on the adaxial and the abaxial sides. Functional Plant Biology 2020; 47(7): 639-50. https://doi.org/10.1071/FP19352

[54] Slaton MR, Raymond Hunt Jr E, Smith WK. Estimating near-infrared leaf reflectance from leaf structural characteristics. American Journal of Botany 2001; 88(2): 278-84. https://doi.org/10.2307/2657019

[55] Nishio JN, Sun J, Vogelmann TC. Carbon fixation gradients across spinach leaves do not follow internal light gradients. The Plant Cell 1993; 5(8): 953-61. https://doi.org/10.2307/3869663

[56] Driscoll SP, Prins A, Olmos E, Kunert KJ, Foyer CH. Specification of adaxial and abaxial stomata, epidermal structure and photosynthesis to CO2 enrichment in maize leaves. Journal of Experimental Botany 2006; 57(2): 381-90. https://doi.org/10.1093/jxb/erj030

[57] Wall S, Vialet-Chabrand S, Davey P, Van Rie J, Galle A, Cockram J, Lawson T. Stomata on the abaxial and adaxial leaf surfaces contribute differently to leaf gas exchange and photosynthesis in wheat. New Phytologist 2022; 235(5): 1743-56. https://doi.org/10.1111/nph.18257

[58] Zhang ZS, Li YT, Gao HY, Yang C, Meng QW. Characterization of photosynthetic gas exchange in leaves under simulated adaxial and abaxial surfaces alternant irradiation. Scientific Reports 2016; 6(1): 26963. https://doi.org/10.1038/srep26963